Signal Processing of Elastic Surface Waves for Localizing Buried Land Mines*

A. Behboodian, W. R. Scott, Jr. and J. H. McClellan
School of Electrical and Computer Engineering
Georgia Institute of Technology
Atlanta, Georgia 30332-0250
behbood@ece.gatech.edu

Abstract

A system that uses elastic surface waves and electromagnetic waves has been developed to detect buried land mines. In this paper an algorithm based on local spatial frequency analysis is presented to illustrate the dispersive effect of the land mine on the acoustic wave and to estimate the wave velocity as a function of position and temporal frequency. In addition, an imaging algorithm is presented which calculates the reflected energy and generates a two-dimensional image that localizes the buried mines.

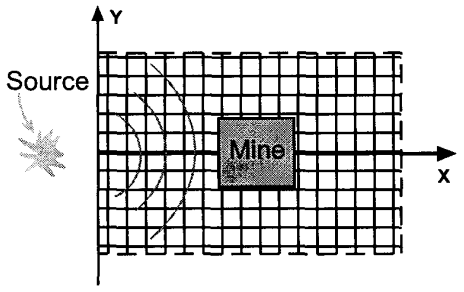

Figure 1. Top view of the experimental system.

1. Introduction

A laboratory system which uses both elastic and electromagnetic waves has been designed and constructed to locate buried mines, metallic as well as nonmetallic [3, 2]. The top view of this experimental system is shown in Fig. 1. An elastic source induces elastic waves into the ground causing both the earth and the mine to vibrate. An electromagnetic radar, designed to measure surface displacements as small as 1 nm, is used to detect these vibrations. The system takes samples on a uniform rectangular grid of discrete positions. The grid consists of 41 points in the y direction spaced 2cm apart and 121 points in the x direction spaced 1cm apart.

The characteristics of the vibrations will differ with the proximity to the mine. Mines have mechanical properties that are significantly different from soil and typical sources of clutter. The shear wave velocity is approximately 10 times higher in mines than in the ground. In addition, the structure of the mine gives rise to a structural resonance not found in other forms of clutter. In this paper signal processing algorithms have been developed to exploit these and other physical phenomena to locate buried mines. The velocity of the elastic wave is estimated locally and depth information is extracted from the data collected over the surface. By exploiting both the elastic wave reflected from the mine and the mechanical resonances induced in the mine, an imaging algorithm was developed which can localize plastic mines as small as 8cm in diameter. These plastic mines cannot be reliably detected with any of the existing methods.

*This work is supported in part under the OSD MURI program by the US Army Research Office under contract DAAH04-96-1-0048

2. Local Wave Velocity Estimation

An important physical property of the elastic surface waves is that waves with lower temporal frequencies penetrate deeper into the ground than waves with higher temporal frequencies [1]. Also the velocity of the elastic wave is higher in the mine than in the surrounding soil. Hence one can expect that waves with low temporal frequencies which penetrate deep enough to hit the buried mine travel faster in the proximity of the mine than waves with higher temporal frequencies. This is a dispersive effect of the buried mine on the elastic waves.

To compute a local estimate of velocity, we should first decompose the collected data, $s(x, y, t)$, into different temporal frequencies. This is done by Fourier transforming the

0-7803-5700-0/99/$10.00©1999 IEEE

data in the time domain. The resulting data set, $S(x, y, f)$, which depends on the spatial domains, x, y, and on the temporal frequency f is then processed separately for each temporal frequency. Depth information can be inferred from this transformed data because penetration depth is proportional to temporal frequency. However, note that while the higher temporal frequencies get affected only by the upper levels of the ground, the lower temporal frequencies get affected by both the upper levels and the lower levels of the ground. Hence the velocity which we determine for the lower temporal frequencies is not the velocity at a particular depth but a weighted average of the depth dependent velocity profile. The average velocity is frequency dependent because the penetration depth of the surface wave is frequency dependent.

To show the dispersive effect of the mine we process a slice of the transformed data, $S(x, y, f)$, at a temporal frequency of 430Hz. The wave at this temporal frequency penetrates deep enough to reach the mine which is buried 5cm under the surface. A spatial-spatial frequency analysis is performed on $S(x, y, 430)$ using a two-dimensional, sliding, rectangular window of 6cm height and 3cm width (this is 3×3 sample window). The two-dimensional Fourier transform of the windowed data is taken. The location where the maximum of the absolute value of the Fourier transform occurs is an estimate of the dominant wave number in the windowed region. Knowing the temporal frequency, one can find the localized velocity in that region by dividing the temporal frequency in rad/s by the magnitude of the wave number in rad/m. Fig. 2 shows the processing result of a data set collected over a $30 \times 30 \times 10$cm simulated mine, buried 5cm deep under the ground. The arrows in the figure depict the wavenumber vector. Only the forward going waves are shown. In this figure the source is located approximately at $(x = -30, y = 0)$. It can be seen that in the area between the source and the mine the wave propagates almost radially from the source. Over the mine the velocity of the wave increases and hence the magnitude of the wavenumber vectors become smaller. After passing the mine the wave fill in the region behind the mine. Some perturbations at the edges of the figure are mainly due to reflections of the wave off the walls of the tank in which the mine is buried.

In another processing, a two-dimensional slice of the data over the line $y = 0$ in Fig. 1 (this is $s(x, 0, t)$) was analyzed for depth information. First, we take the Fourier transform of the data in the time domain. At each temporal frequency, the spectrogram of the data is calculated in the spatial domain with a Hanning window of length 15cm (a length of 15 samples) with an overlapping of 14cm. At each window location, the spatial frequency where the maximum of the magnitude of the Fourier transform occurs is the dominant wavenumber. The velocity can hence be calculated

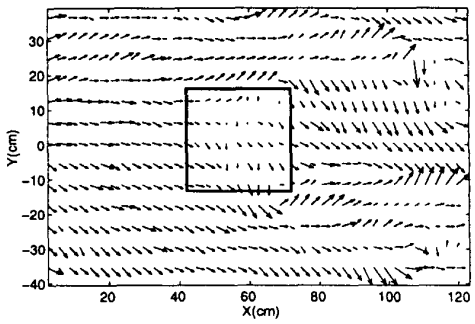

Figure 2. Wavenumber vectors at a temporal frequency of 430Hz over a buried anti-tank mine.

knowing the temporal frequency. Results over a range of temporal frequencies is shown in Fig. 3 for two different data sets. In Fig. 3(a) a simulated $30 \times 30 \times 10$cm anti-tank mine is buried 5cm under the ground whereas in Fig. 3(b) the same mine is buried 10cm under the ground. It can be seen from the figure that waves with high temporal frequencies are less affected by the presence of the mine. This is because these waves do not penetrate as much in the ground to reach the mine. Waves with medium temporal frequencies get affected the most and their velocity increases sharply over the mine. Finally, it is seen that waves with low temporal frequencies are also less affected by the presence of the mine. The reason is two fold. On one hand, we know that these waves have large wave lengths and hence have less interaction with the mine. On the other hand, these waves penetrate much deeper into the ground. Hence the presence of a 10cm thick mine does not affect the velocity of the low frequency waves as much as it affects the velocity of the medium frequency waves. Note in the figure that higher range of frequencies get less affected by the deeper mine.

3. Imaging Algorithm

In addition to processing the data to estimate the velocity of the elastic wave and infer depth information from the data, we have also developed an algorithm to image the data. The algorithm exploits two basic properties at the same time. The first property is that incident elastic wave, traveling at the surface of the ground gets reflected back upon arriving at a buried object. This property is most useful for the case of large mines. The reflection off the small mines such as anti-personnel mines is small and hard to distinguish from the background noise. Another fundamental property of mines is their structural resonance. Elastic

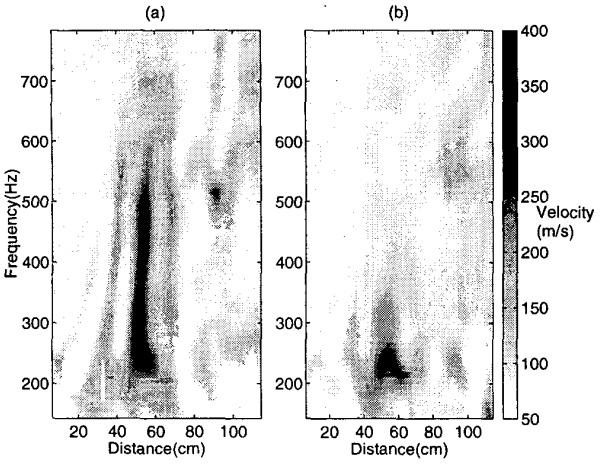

Figure 3. Temporal-Spatial analysis of collected data over y = 0. (a) 5cm deep. (b) 10cm deep.

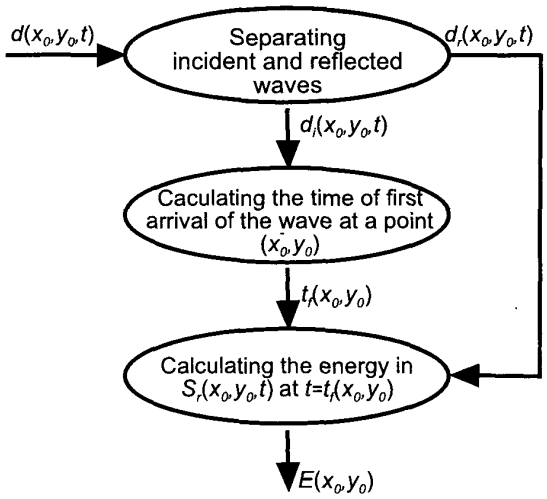

Figure 4. The three steps involved in formation of an image.

waves, upon arriving at the mine, cause the mine to resonate [2]. The resonance not only enables us to locate small mines, but also gives us the ability to distinguish between clutter such as stones and small mines. An explanation of how the imaging algorithm works comes next.

One way to define a reflector is that it is located at a point where the first arrival of the incident wave is time coincident with the reflected wave. The resonance also starts at the first arrival of the wave to the mine. The basic idea behind our algorithm is to calculate the time it takes for the wave to get to a point on the surface and then calculate the energy in the reflection and resonance near that point. To exploit this idea we proceed in three steps depicted in Fig. 4. In the first step, we separate the incident and reflected waves. The separation process can readily be explained in the $\omega - k$ domain. In two dimensions, the incident wave has energy in the first and third quadrants in the $\omega - k_x$ domain while the reflected wave has energy in the second and fourth quadrant. Fig. 5 shows the frequency transform of the data collected over the line $y = 0$ in Fig. 1. Obviously the energy of the reflected wave is less than the energy of the incident wave which is also seen from the figure. The first and third quadrants are filtered out leaving us with the reflected wave.

In the second step, we find the time $t_f(x, y)$, when the incident wave first arrives at a point (x, y) on the surface. This requires us to have an estimate of the wave velocity. Here, we use an estimate of the bulk velocity by simply measuring the slope of the traveling wavelet in the $x - t$ domain of the collected data. The $x - t$ domain data is shown in Fig. 6 with a line fitted to the incident wave. The processes involved in the last step of the imaging algorithm are shown in Fig. 7. For each point (x_0, y_0) on the surface we calculate the energy of the reflected wave near $t_f(x_0, y_0)$. This energy is obtained by calculating the energy of a windowed portion of the time signal for that location. The window is centered at the time it takes for the traveling wave to reach this location, which was calculated in the previous step. A triangular window is used. The energy calculated is also compensated for the energy loss by multiplying the result for each point by the squared distance of the source to that point. Results of the imaging algorithm is shown in Fig. 8 and Fig. 9. In Fig. 8 the simulated anti-tank mine is buried 5cm under the ground centered at $x = 55, y = 0$. Here the mine does not have a structural resonance and the imaging algorithm is mainly exploiting the reflection of the wave off the mine. An actual mine will also have structural resonances which should improve the image. In Fig. 9 a small mine (8cm in diameter) is buried about 2cm deep in the ground centered at $x = 50, y = 0$ along with rocks and sticks. Here the reflection is small and the algorithm is basically locating the energy of the resonance which is also a signature to distinguish the mine from the clutter.

4. Conclusion

Signal processing algorithms have been developed to estimate the localized velocity of the elastic wave, inferring depth information and imaging the data collected by an electro-acoustic system. Examples of the algorithms have been presented. Using the imaging algorithm, one can lo-

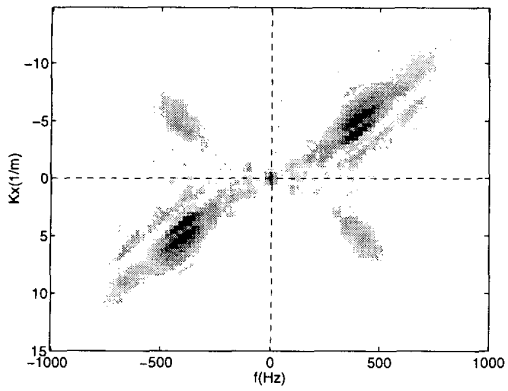

Figure 5. Two-dimensional Fourier transform of the data collected along $y = 0$.

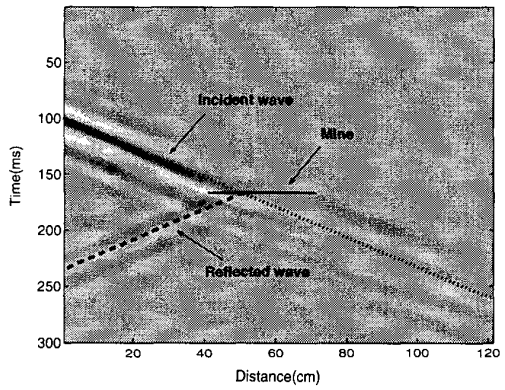

Figure 6. Data collected at $y = 0$.

calize small mines and distinguish them from the clutter. Research in increasing the resolution of the images by a better estimation of different parameters is currently being pursued.

References

[1] K. F. Graph. *Wave Motion in Elastic Solids.* Dover Publications, 1975.

[2] W. R. Scott, Jr. and J. S. Martin. Experimental investigation of the acousto-electromagnetic sensor for locating land mines. *Proceedings of the SPIE: 1999 Annual International Symposium on Aerospace/Defense Sensing, Simulation, and Controls, Orlando, FL,* 3710:204–214, April 1999.

[3] W. R. Scott, Jr., C. Schroeder, and J. S. Martin. A hybrid acoustic/electromagnetic technique for locating land mines. *Proceedings of the 1998 International Geoscience and Remote Sensing Symposium,Seattle, Washington,* pages 216–218, July 1998.

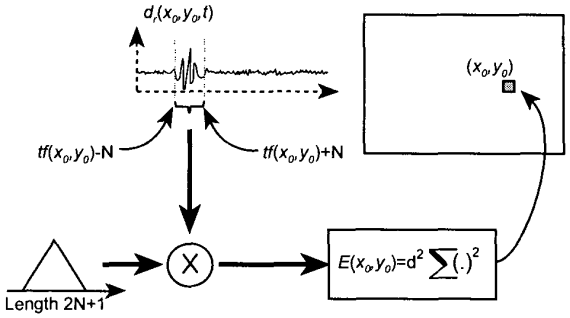

Figure 7. Process involved in the last step of the imaging algorithm.

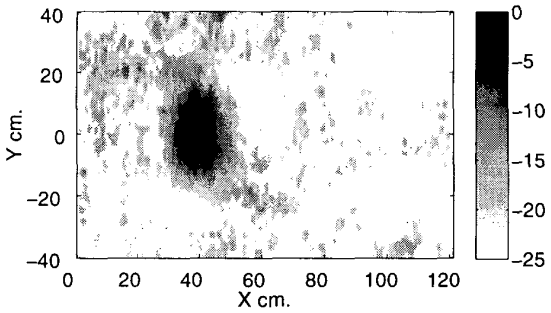

Figure 8. A 25dB image of an anti-tank mine obtained by the imaging algorithm.

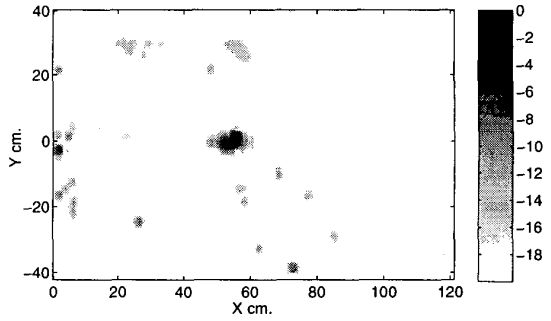

Figure 9. A 20dB image of an anti-personnel mine obtained by the imaging algorithm.